Microscopic Insight into Electron-Induced Dissociation of Aromatic Molecules on Ice

Philipp Auburger,[1] Ishita Kemeny,[2] Cord Bertram,[2,3] Manuel Ligges,[2] Michel Bockstedte,[1,4] Uwe Bovensiepen,[2] and Karina Morgenstern[3]

[1]*Solid State Theory, Friedrich-Alexander University Erlangen-Nürnberg, Staudstr. 7B2, D-91058 Erlangen, Germany*
[2]*Faculty of Physics, University of Duisburg-Essen, Lotharstr. 1, D-47057 Duisburg, Germany*
[3]*Physical Chemistry I, Ruhr-Universität Bochum, Universitätsstr. 150, D-44801 Bochum, Germany*
[4]*Department of Chemistry and Physics of Materials, Paris-Lodron University Salzburg, Jakob-Haringer-Str. 2a, A-5020 Salzburg, Austria*

(Received 24 May 2018; published 13 November 2018)

We use scanning tunneling microscopy, photoelectron spectroscopy, and *ab initio* calculations to investigate the electron-induced dissociation of halogenated benzene molecules adsorbed on ice. Dissociation of halobenzene is triggered by delocalized excess electrons attaching to the π^* orbitals of the halobenzenes from where they are transferred to σ^* orbitals. The latter orbitals provide a dissociative potential surface. Adsorption on ice sufficiently lowers the energy barrier for the transfer between the orbitals to facilitate dissociation of bromo- and chloro- but not of flourobenzene at cryogenic temperatures. Our results shed light on the influence of environmentally important ice particles on the reactivity of halogenated aromatic molecules.

DOI: 10.1103/PhysRevLett.121.206001

Photo-induced dissociation of gas phase molecules [1] is substantially enhanced on water-ice particles [2]. This reaction is highly relevant for atmospheric chemistry [3,4], which often proceeds on ice-covered dust particles. By this reaction, dissociation of halogen containing organic compounds has a large environmental relevance due to the release of radicals [5], e.g., chlorine and bromine that impact hydrocarbon, ozone, and cloud concentrations in the atmosphere.

Organic compounds adsorb on ice surfaces via their interaction with dangling OH groups that are not engaged in ice related hydrogen bonding [6]. Such an adsorption leads to a measurable shift of the optical absorption spectrum for a variety of organic pollutants [5]. Electron attachment to molecules adsorbed on solid substrates mediates chemical reactions via the formation of transient ions. Thus, photoexcited excess electrons may dissociate the adsorbed molecules [7]. In the atmosphere, these electrons originate either from an impact of high energy particles with ice [2] or from sunlight induced photo-excitation of in-gap states in doped ice [8]. The electrons may exist in ice in two forms: either delocalized or localized as so-called solvated electrons [9,10] (Fig. 1). Despite the relevance of such processes in environmental and atmospheric science, they remain poorly understood.

A dependence of reaction rate on the environment was shown for haloalkanes adsorbed on various substrates [2,11–14]. A coadsorption with molecules such as water or methanol evidenced cooperative effects among the polar molecules [14,15], though not yet giving microscopic insights. In this class of adsorbed molecules, barrierless dissociation is induced by an electron injected into a σ^* antibonding orbital [13]. It was demonstrated that interactions with its surroundings influences the orbital [16]. What remains open, even in this rather simple case, is how far these various couplings of molecule, substrate and electronic interaction among the constituents compete or cooperate in the dissociation process itself.

The potential landscape provided by antibonding orbitals is not always as simple as the one of haloalkanes. Electron-induced reactions were studied for wider and more complex classes of molecules in the gas phase. For haloarene molecules, where a halogen is directly bound to an aromatic ring, the electron is attached initially to a non-dissociative potential surface and is transferred subsequently to the dissociative one [17]. However, such molecules were studied only rarely after adsorption at the microscopic level [18,19]. Moreover, the influence of the environment on the reaction mechanism remains rather unexplored at this scale.

In this Letter we reveal the elementary steps leading to the dissociation of halobenzene adsorbed on ice (C_6H_5X/D_2O with $X = F$, Cl, Br) after electron attachment. We demonstrate that hot electrons, excited by ultraviolet light in a Cu(111) electrode, propagate in Bloch-like states through adsorbed D_2O clusters untill they attach to the π^* antibonding orbitals of the halobenzene, from where they transfer to the dissociative σ^* orbital. The interaction of the halobenzenes with the water molecules determines the dissociation yield. On a broader range, our results give physical insight into the influence of hydration on reactivity.

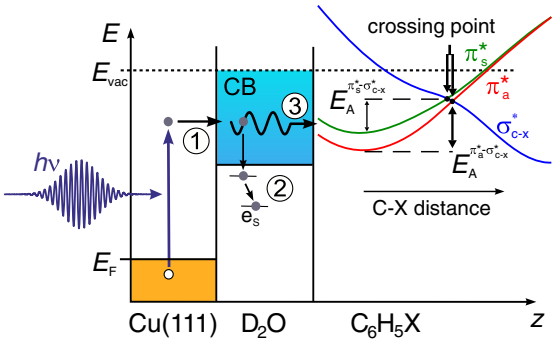

FIG. 1. Model for the photo-induced electron attachment to halobenzene (C_6H_5X, $X = $ F, Cl, Br): (1) injection of photoexcited electrons into the ice conduction band, (2) electron solvation in localized states, (3) propagation of delocalized electrons and attachment to molecular π^* orbitals, (right) generic potential surfaces of the halobenzene, see text.

We arrive at these conclusions by developing and verifying a model, shown in Fig. 1, to describe the interaction of adsorbed molecules with photoexcited excess electrons at the ice surface. It is based on photoexcitation and photoinjection of hot electrons into the ice conduction band, where the electron could either localize and form solvated electrons e_s^- (e.g., [9,10,20–24]) or propagate in Bloch-like or presolvated states [13,14]. Subsequently, the electrons can attach to individual molecules and induce dissociation according to

$$C_6H_5X + e^- \leftrightarrow C_6H_5X^{*-} \leftrightarrow C_6H_5 + X^-. \qquad (1)$$

Our model provides a microscopic understanding how ice enhances halobenzene dissociation. We employ the complementary methods of scanning tunneling microscopy (STM), two-photon photoelectron spectroscopy (2PPE), and *ab initio* theory to substantiate our model.

For modeling we employ density functional theory (DFT) with semilocal (PBE) and hybrid (PBE0) functionals as well as many body perturbation theory (GW and BSE) as implemented in the VASP package (cf. [25]) to address structural, electronic, and photophysical properties of the adsorbate-ice system. Details on the realization of the ice surface and the different levels of theory are given in the Supplemental Material [26].

The experiments are performed in two separate ultrahigh vacuum chambers with comparable facilities for the preparation of surfaces and molecule deposition. After standard cleaning cycles of Cu(111) single crystals, approximately 1 BL and 4 BL (bilayers) of amorphous ice (D_2O) are deposited at liquid nitrogen temperature, for STM and photoemission experiments, respectively. Given in units of a full monolayer (ML) on the bare Cu(111), approximately 0.4 ML and 1 ML of halobenzene molecules are deposited at liquid nitrogen temperature for STM and photoemission experiments, respectively.

For the STM experiments (at 7.5 K, 0.1 V, and 1 to 5 pA), the tunneling junction is illuminated for 10 h by a frequency-doubled supercontinuum laser (NKT Photonics, 77.8 MHz, 10 ps, p polarized). At 326, 330, and 400 nm the illumination fluences F are 2.3 pJ/cm^2, 20 pJ/cm^2, and 230 pJ/cm^2, respectively.

2PPE combines photoexcitation at ultraviolet wavelength and sensitive work function determination [41]. The experiments are performed using a Ti:sapphire laser amplifier (Coherent RegA 9040, repetition rate: 250 kHz). A noncollinear optical parametric amplifier generates light at a wavelength of 327 nm in a fluence range from 0.5 to 10 μJ/cm^2. The 2PPE spectrum is analyzed by an electron time of flight spectrometer with an energy resolution of 10 meV at $E_{\mathrm{kin}} = 1$ eV [42].

The different fluences for the two different setups are compensated by adapting the illumination times. This is a reliable procedure because all photoinduced processes are found to be linear in F.

We start by exploring how adsorption on ice could alter dissociation in theory. We model the energy landscape of the halobenzenes in the gas phase and investigate changes induced by adsorption on an idealized ice surface and at several surface defect sites within our *ab initio* approach [26]. In the gas phase, the dissociation of halobenzenes is initiated by the formation of a metastable transient anion $C_6H_5X^{*-}$ via the occupation of an antibonding orbital, a symmetric or antisymmetric π^*, or a σ^* orbital [Fig. 2(a)] [1,17]. The transient ion dissociates in a barrierless manner in the latter case. The dissociation of the halogen is facilitated by a node of the σ^* orbital located at the C-X bond [Fig. 2(a), inset]. As this orbital is quite high in energy, a low-energy pathway for dissociation proceeds via the occupation of one of the π^* orbitals and subsequent transition to the σ^* orbital at the conical intersection between the π^* and σ^* potential energy surfaces after some bond elongation [Figs. 1, 2(a)]. In this case, an energy barrier E_A has to be overcome. The amorphous surface, on

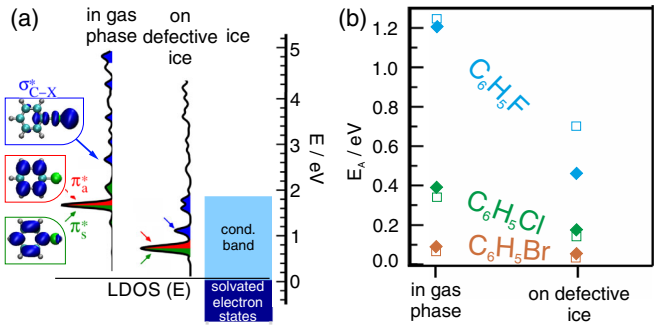

FIG. 2. Modelling of C_6H_5X: (a) LDOS for C_6H_5Cl in gas phase and adsorbed on defective ice with orbital shapes as insets, (b) activation energies E_A for different halobenzenes in gas phase and adsorbed on defective ice; open symbols denote $E_A^{\pi_a^*-\sigma^*}$; filled symbols denote $E_A^{\pi_s^*-\sigma^*}$.

which we perform the dissociation experiments, can be more efficiently modeled by defects at the idealized surface than by just an idealized surface. Furthermore, defects are found in STM experiments to serve as anchor sites for the halobenzene molecules at low coverage (not shown) and thus set the environment where dissociation proceeds.

Defect sites differ from idealized surface configurations by either missing [43] or reoriented [44] water molecules or a combination of both, thus providing dangling OH groups for interactions with charged particles, discussed so far as traps for electrons. Trapping of electrons is confirmed by our calculations, which reveals an energy gain of up to 1 eV through the attractive interaction of the electrons with the positive partial charges of the dangling OH groups (for details, see Ref. [26]).

Though differing quantitatively, the calculated shift of orbital energies at all anchor sites and the idealized ice are qualitatively equivalent, suggesting the same for the energy barrier. A deliberately chosen orientation defect is thus taken below as a representative example of a strong anchor site [27]. The adsorption of halobenzenes at such an anchor site is favored by the same attractive interaction that stabilizes and solvates electrons. In the present case, the negative partial halogen charge is stabilized by the rearrangement of OH groups [26]. Adsorption redshifts the antibonding orbitals of the halobenzenes into the region of the ice conduction band edge, still being well above solvated electron states as evidenced by the local density of states [LDOS, Fig. 2(a)]. This redshift of the antibonding orbitals results from the attractive interaction of the polar molecule with the positive partial charges of the dangling OH groups. It facilitates electron attachment and will thus increase dissociation rates. The redshift increases along the halogenated molecules series (C_6H_5X, X = F, Cl, Br); i.e., the benzenes with halogens of larger mass and with lower electron affinity shift the orbitals to lower energy [26]. Moreover, the activation energy to the crossing point E_A is reduced upon adsorption [45], again even more for halogens of lower electron affinity [Fig. 2(b)]. The halogen-specific reduction in energy should translate into halogen-specific dissociation rates being larger for halogens of lower electron affinity.

Our calculations reveal that the halobenzene molecules are trapped at anchor sites with an abundance of dangling OH groups. Thus, the same sites that solvate electrons also anchor the polar molecules because of their partial charges. However, solvated electrons are unable to initiate dissociation because of their positioning below the conduction band of ice [Fig. 2(a)]. The dissociation at the anchor sites can thus only be initiated by the electrons delocalized in the ice conduction band [46] as sketched on the top in Fig. 1.

In order to verify this theoretical picture experimentally, we adsorb halobenzenes onto ice nanoparticles supported on Cu(111). The copper electrode serves as an electron source, which allows the transferring of delocalized electrons into the conduction band of ice upon excitation by ultraviolet light [22]. Here we excite this system by a photon energy below 3.8 eV, too low to photoexcite and dissociate the molecules in the gas phase and, according to our calculation, also at the ice surface [26]. This low energy ensures that no direct photodissociation falsifies our measurements and all processes reported below originate from electrons transferred to the conduction band of ice.

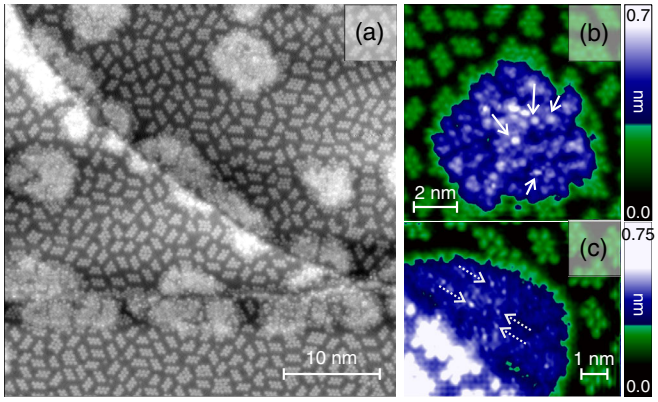

FIG. 3. Identification of adsorption and reaction events by STM for chlorobenzene on amorphous ice, 0.1 V, 5 pA (a), (b) before and (c) after illumination at 5.2×10^5 photons/molecule, 326 nm; solid and dashed arrows point to adsorbed and dissociated molecules, respectively.

In the STM images, the halobenzene molecules are easily identified on the pristine Cu(111) surface as ellipsoidal protrusions forming regular clusters [Fig. 3(a)]. On the amorphous ice surface both, the water and the halobenzene molecules appear as blue to white protrusions at the chosen color scale in [Fig. 3(b)], as they are at the same height. Some of the halobenzenes are easily identified as they are imaged at a larger height than any water in the corresponding structure, some because of their larger diameter [marked by arrows in Fig. 3(b)]. However, more commonly, many molecules can only be identified in retrospect after illumination.

Illumination substantially changes the imaging of the adsorbates on the ice surfaces [Fig. 3(c)]. Halobenzenes are easily moved by the STM tip before illumination, but not after illumination. The more tightly bonded species interacts characteristically with the tip at all feasible tunneling parameters, which leads to protrusions that are much sharper and of larger apparent height [Fig. 3(c)]. Such species are observed after illumination with both 400 nm and 326/330 nm wavelengths for both chlorobenzene and bromobenzene. They are neither observed before illumination nor after illumination of the native ice without halobenzene nor for the molecules on the pristine Cu surface. The STM experiments thus imply that the ice promotes a reaction that is not possible on the pristine surface under the illumination conditions of our measurements.

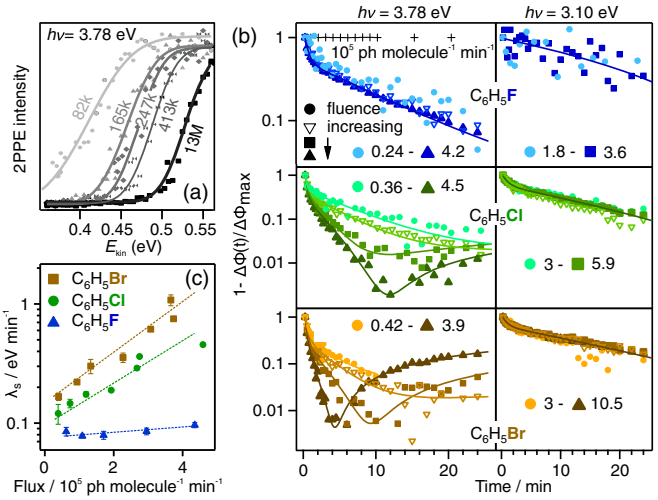

FIG. 4. Halogen specific reactivity on amorphous ice nanoclusters: (a) low energy cutoff of two-photon photoemission spectra using 327 nm illumination for indicated photon dose; lines are fits of an error function for determination of the work function Φ. (b) Relative change of work function vs illumination time on logarithmic scale obtained from low energy cutoff (see panel a) for different photon fluxes, photon energy as indicated on top, and halobenzenes; plus signs (+) for $C_6H_5F/Cu(111)$ without ice; lines are multiexponential fits to determine the rates of change λ in $\Delta\Phi$. (c) Slow rate of change λ_S vs flux for the series of halobenzenes; dashed lines guide the eye.

In order to prove that the observed changes are related to dissociation, we measure the shift of the Cl(2p) orbital in x-ray photoemission [26] as well as the work function change $\Delta\Phi = \Phi(t) - \Phi(t = 0)$ induced by the illumination of halobenzenes adsorbed on amorphous ice structures. While the shift of Cl(2p) to higher binding energy proves that the molecules dissociate upon illumination in agreement with literature values [34], the work function change, measured as the low energy cut off of the 2PPE spectrum [Fig. 4(a)] is an indicator for the amount of halogen ions after dissociation, because it is determined by the charge distribution along the surface normal. Indeed, the low energy cut off shifts to higher kinetic energy with photoexposure time [Fig. 4(a)] corresponding to a work function increase. The relative changes for different photon energy, halobenzenes, and fluence are normalized to the maximum change $\Delta\Phi_{max}$ and depicted in Fig. 4(b). Such work function changes are not observed for halobenzenes adsorbed directly on the metal surface, e.g., $C_6H_5F/Cu(111)$ [Fig. 4(b), plus sign], confirming the STM observation and the theoretical prediction. Evidently, ice promotes dissociation.

Our model is further confirmed by the significant differences in work function change along the halogen series [Fig. 4(b)]. While, for C_6H_5F, a biexponential increase in the relative work function changes with illumination time, it does not change with photon flux; we observe flux-dependent variations for C_6H_5Cl and C_6H_5Br at a photon energy of 3.78 eV. For these two heavier halogens, their initial work function change is accelerated with increasing photon flux for the larger photon energy and the sign of change inverses at later times. The multiexponential fit of the time-dependent work function (cf. [26]) gives a slow molecule-dependent rate λ_s after an initial fast molecule-independent rate; the slow rate is plotted in Fig. 4(c). Flux-independent photoinduced work function changes in time indicate, in general, a buildup of a photostationary state, in which for instance attachment and detachment of electrons to the adsorbate lead to an equilibrium density of transient ions ($C_6H_5X^{*-}$) without dissociation. For C_6H_5F, the flux dependence of the slow rate of work function change λ_s is weak. We conclude that the observation for C_6H_5F indicates the formation of such transient ions only. Indeed, for fluorobenzene, the activation energy for dissociation [Fig. 2(b)] is much larger than the thermal energy provided in the experiment, here 90 K, such that dissociation should not take place, as observed. In contrast, a flux dependence as observed for the two heavier halogens suggests a permanent change of the surface. Here, it indicates the formation of a C_6H_5 radical and X^- and thus dissociation. The smaller dissociation rate of chlorobenzene as compared to bromobenzene agrees well with the calculated trend in activation energy [Fig. 2(b)]. The inversion of the work function change at later times is related to the consumption of the available native halobenzenes by dissociation reducing the number of transient ions. Our conclusions are verified by experiments using a photon energy of 3.1 eV, which is too low to induce dissociation [Fig. 2(a)], and indeed the fluence dependent behavior of $\Delta\Phi$ [Fig. 4(b)] serving as a fingerprint of dissociation is absent. Our experimental results thus confirm the molecular scale picture developed above.

In conclusion, ice mediates dissociative electron attachment to halogenated aryls by redshifting the active orbitals and by lowering the activation energy at the conical intersection between antibonding orbitals. Such a cooperative effect on a reaction probability should be a universal property of polar molecules and emphasizes the active role of polar solvents in electron-induced chemical reactions. The proposed mechanism should not only be valid for atmospheric chemistry and astrophysics, where the investigated ice structures exist at cryogenic temperatures, but has further implications in fields as diverse as electrochemistry and biology, where flexible solvation shells of similar structure exist transiently but long enough for an electron-induced reaction to occur.

The authors acknowledge financial support by the Deutsche Forschungsgemeinschaft under Grants No. BO1841/3-1, No. BO1823/5-1, and No. MO960/18-1 and the Cluster of Excellence RESOLV (EXC 1069). For computer time we thank the Research Center Jülich (HER140) and the FAU Erlangen-Nürnberg (HPC cluster of RRZE). We thank Ting-Chieh Hung, PCI, RUB, for supporting the XPS measurements.

[1] O. Ingolfsson, F. Weik, and E. Illenberger, Int. J. Mass Spectrom. Ion Processes **155**, 1 (1996).
[2] Q.-B. Lu and L. Sanche, Phys. Rev. Lett. **87**, 078501 (2001).
[3] M. Dameris, Angew. Chem. **49**, 8092 (2010).
[4] C. George, M. Ammann, B. D'Anna, D. J. Donaldson, and S. A. Nizkorodov, Chem. Rev. **115**, 4218 (2015).
[5] I. J. George and J. P. D. Abbatt, Nat. Chem. **2**, 713 (2010).
[6] N. S. Holmes and J. R. Sodeau, J. Phys. Chem. A **103**, 4673 (1999); A. Borodin, O. Hofft, U. Kahnert, V. Kempter, S. Krischok, and M. O. Abou-Helal, J. Chem. Phys. **120**, 5407 (2004).
[7] B. C. Garret *et al.*, Chem. Soc. Rev. **105**, 355 (2005).
[8] I. V. Hertel, C. Huglin, C. Nitsch, and C. P. Schulz, Phys. Rev. Lett. **67**, 1767 (1991); T. Vondrak, J. M. C. Plane, and S. R. Meech, J. Chem. Phys. **125**, 224702 (2006); V. Balzani, G. Bergamini, and P. Ceroni, Angew. Chem. **54**, 11320 (2015).
[9] E. J. Hart and J. W. Boag, J. Am. Chem. Soc. **84**, 4090 (1962).
[10] K. R. Siefermann, Y. Liu, E. Lugovoy, O. Link, U. B. M. Faubel, B. Winter, and B. Abel, Nat. Chem. **2**, 274 (2010).
[11] W. W. B. Gergen, H. Nienhaus, and E. McFarland, Science **294**, 2521 (2001).
[12] Q.-B. Lu and L. Sanche, J. Chem. Phys. **120**, 2434 (2004).
[13] C. C. Perry, N. S. Faradzhev, D. H. Fairbrother, and T. E. Madey, Int. Rev. Phys. Chem. **23**, 289 (2004).
[14] E. T. Jensen, Phys. Chem. Chem. Phys. **17**, 9173 (2015).
[15] V. Poterya, J. Kocisek, J. Lengyel, P. Svrckova, A. Pysanenko, D. Hollas, P. Slavicek, and M. Farnik, J. Phys. Chem. A **118**, 4740 (2014).
[16] V. A. Ukraintsev, T. J. Long, T. Gowl, and I. Harrison, J. Chem. Phys. **96**, 9114 (1992).
[17] A. Modelli, Phys. Chem. Chem. Phys. **5**, 2923 (2003).
[18] X. Chen, Q. Kong, J. Polanyi, D. Rogers, and S. So, Surf. Sci. **340**, 224 (1995).
[19] P. A. Sloan and R. E. Palmer, Nature (London) **434**, 367 (2005).
[20] J. R. R. Verlet, A. E. Bragg, A. Kammrath, O. Cheshnovsky, and D. M. Neumark, Science **307**, 93 (2005).
[21] K. Onda, B. Li, J. Zhao, K. D. Jordan, J. Yang, and H. Petek, Science **308**, 1154 (2005).
[22] J. Stähler, M. Mehlhorn, U. Bovensiepen, M. Meyer, D. O. Kusmierek, K. Morgenstern, and M. Wolf, Phys. Rev. Lett. **98**, 206105 (2007).
[23] U. Bovensiepen, C. Gahl, J. Stähler, M. Bockstedte, M. Meyer, F. Baletto, S. Scandolo, X.-Y. Zhu, A. Rubio, and M. Wolf, J. Phys. Chem. C **113**, 979 (2009).
[24] M. P. Coons, Z.-Q. You, and J. M. Herbert, J. Am. Chem. Soc. **138**, 10879 (2016).
[25] M. Shishkin and G. Kresse, Phys. Rev. B **75**, 235102 (2007).
[26] See Supplemental Material at http://link.aps.org/supplemental/10.1103/PhysRevLett.121.206001, which describes details of the experiments and theoretical modelling, XPS experiments, the influence of adsorption on molecular orbitals, image potential effects, and competing dissociation mechanisms, and which includes Refs. [27–40].
[27] M. Mehlhorn and K. Morgenstern, New J. Phys. **11**, 093015 (2009).
[28] M. Mehlhorn and K. Morgenstern, Phys. Rev. Lett. **99**, 246101 (2007).
[29] M. Shishkin and G. Kresse, Phys. Rev. B **75**, 235102 (2007).
[30] T. Sander, E. Maggio, and G. Kresse, Phys. Rev. B **92**, 045209 (2015).
[31] M. Bockstedte, A. Michl, M. Kolb, M. Mehlhorn, and K. Morgenstern, J. Phys. Chem. C **120**, 1097 (2016).
[32] D. Pan, L.-M. Liu, G. A. Tribello, B. Slater, A. Michaelides, and E. Wang, Phys. Rev. Lett. **101**, 155703 (2008).
[33] U. Bovensiepen, C. Gahl, J. Stähler, M. Bockstedte, M. Meyer, F. Baletto, S. Scandolo, X.-Y. Zhu, A. Rubio, and M. Wolf, J. Phys. Chem. C **113**, 979 (2009).
[34] X.-L. Zhou and J. M. White, J. Chem. Phys. **92**, 5612 (1990).
[35] V. A. Ukraintsev, T. J. Long, T. Gowl, and I. Harrison, J. Chem. Phys. **96**, 9114 (1992).
[36] A. Sobolewski and W. Dohmke, Chem. Phys. **259**, 181 (2000).
[37] M. Palmer, T. Ridley, S. Hoffmann, N. C. Jones, M. Coreno, M. de Simone, C. Grazioli, T. Zhang, M. Biczysko, A. Baiardi, and K. Peterson, J. Chem. Phys. **143**, 164303 (2015).
[38] M. Palmer, T. Ridley, S. Hoffmann, N. C. Jones, M. Coreno, M. de Simone, C. Grazioli, T. Zhang, M. Biczysko, A. Baiardi, and K. A. Peterson, J. Chem. Phys. **144**, 124302 (2016).
[39] Y.-J. Liu, P. Persson, and S. Lunell, J. Phys. Chem. A **108**, 2339 (2004).
[40] *CRC Handbook of Chemistry and Physics* edited by J. R. Rumble (CRC Press/Taylor & Francis, Boca Raton, Florida, 2017).
[41] M. Bertin, M. Meyer, J. Staehler, C. Gahl, M. Wolf, and U. Bovensiepen, Faraday Discuss. **141**, 293 (2009).
[42] M. Sandhofer, I. Sklyadneva, V. Sharma, V. M. Trontl, P. Zhou, M. Ligges, R. Heid, K.-P. Bohnen, E. Chulkov, and U. Bovensiepen, J. Electron Spectrosc. Relat. Phenom. **195**, 278 (2014).
[43] M. Watkins, J. VandeVondele, and B. Slater, Proc. Natl. Acad. Sci. U.S.A. **107**, 12429 (2010).
[44] M. Watkins, D. Pan, E. G. Wang, A. Michaelides, J. VandeVondele, and B. Slater, Nat. Mater. **10**, 794 (2011).
[45] Such a reduction of E_A does not arise from image potential in the case of ice grown on metal [26].
[46] Other competing mechanisms are excluded [26].